We are IntechOpen, the world's leading publisher of Open Access books Built by scientists, for scientists

4,800
Open access books available

122,000
International authors and editors

135M
Downloads

Our authors are among the

154
Countries delivered to

TOP 1%
most cited scientists

12.2%
Contributors from top 500 universities

CLARIVATE ANALYTICS BOOK CITATION INDEX INDEXED

WEB OF SCIENCE™

Selection of our books indexed in the Book Citation Index in Web of Science™ Core Collection (BKCI)

Interested in publishing with us?
Contact book.department@intechopen.com

Numbers displayed above are based on latest data collected.
For more information visit www.intechopen.com

Chapter 2

Strike-Slip Basin – Its Configuration and Sedimentary Facies

Atsushi Noda

Additional information is available at the end of the chapter

http://dx.doi.org/10.5772/56593

1. Introduction

Plate convergent margins are areas of concentrated lithospheric stress. They include areas of compression accompanied by thrusting, mountain building, and related foreland/forearc basin development, and also areas of strike-slip movement associated with transpressional uplift, transtensional subsidence, or pure strike-slip displacement. The degree of shortening and uplift or extension and subsidence depends on the modes of convergence between oceanic plates, island arcs, and continental crusts. Strike-slip faulting is one of the most important mechanisms of sedimentary basin formation at plate convergent margins, where localized extension can cause topographic depressions. Sedimentary strata deposited in these basins record the history of lithospheric response to the convergence.

Sedimentary successions of archetypal examples of strike-slip basins, such as the Ridge Basin in California, have been characterized in terms of the dominance of axial sediment supply and continuous depocenter migration in a direction opposite to that of the sediment supply [1]. Their basin lengths are typically about three times longer than the basin widths [2]. The Izumi Group of the Cretaceous turbidite successions in southwestern Japan [e.g., 3 and references therein] has the same characteristics in the sedimentary succession as the Ridge Basin, and is therefore considered to contain strata that were deposited in a strike-slip basin. However, the basin geometry is quite different from that of the Ridge Basin, whose shape is more elongated with a length of more than 300 km and a width of less than 20 km, and whose southern margin has been truncated by post-depositional strike-slip fault displacement. Strike-slip basins thus present a wide diversity in terms of their geometry, evolution, and filling processes.

Since many local examples were collected after the 1980s [4], advanced research techniques including subsurface exploration including seismic survey and borehole drilling [e.g., 5], analog experiment [e.g., 6], and numerical simulation [e.g., 7] revealed that basin formation

and filling processes were not simple but variable. In this paper, I try to review some of representative strike-slip basins along convergent margins, especially focusing on basin formation and filling processes, as the first step for comprehensive understandings of the tectono-sedimentary evolution in strike-slip basins.

2. Strike-slip faults

Much research has been published regarding the classification and terminology of strike-slip faults [e.g., 8–12]. Here, I use three tectonic settings as a basis for classifying strike-slip faults along convergent plate margins: subduction, continental collision, and plate-boundary transform zones.

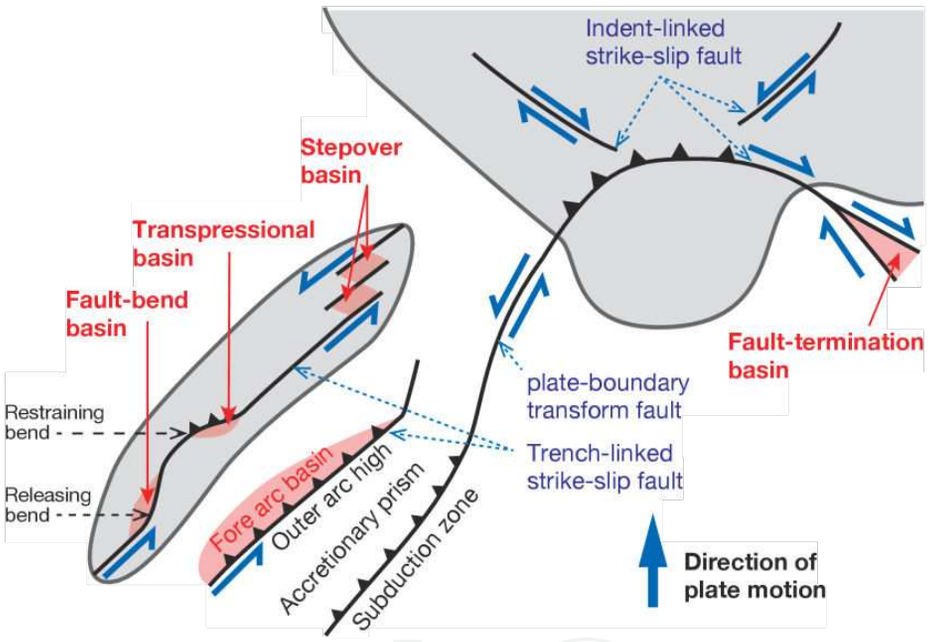

Figure 1. Tectonic settings of strike-slip faults and related strike-slip basins

2.1. Subduction zone

Subduction zones, where oceanic plates obliquely subduct underneath continental or island arc crusts, are sometimes accompanied by strike-slip faults separating elongate forearc slivers from continental margins or island arcs. This type of strike-slip fault is referred to as a trench-linked [9] or trench-parallel [13] strike-slip fault (Figure 1).

Trench-linked strike-slip faults lie parallel to the trench in the accommodating part of the trench-parallel component of oblique convergence of subducting plates [14–16]. The basic principle is considered to be that a trench-linked strike-slip fault is able to concentrate shear in a much more efficient way than distributing shear across the much larger and more gently dipping interface of the subducting plate. Therefore, the low dip angles and high friction

http://dx.doi.org/10.5772/56593

coefficients of subduction zones favor slip on vertical strike-slip faults rather than on gently dipping slabs [9].

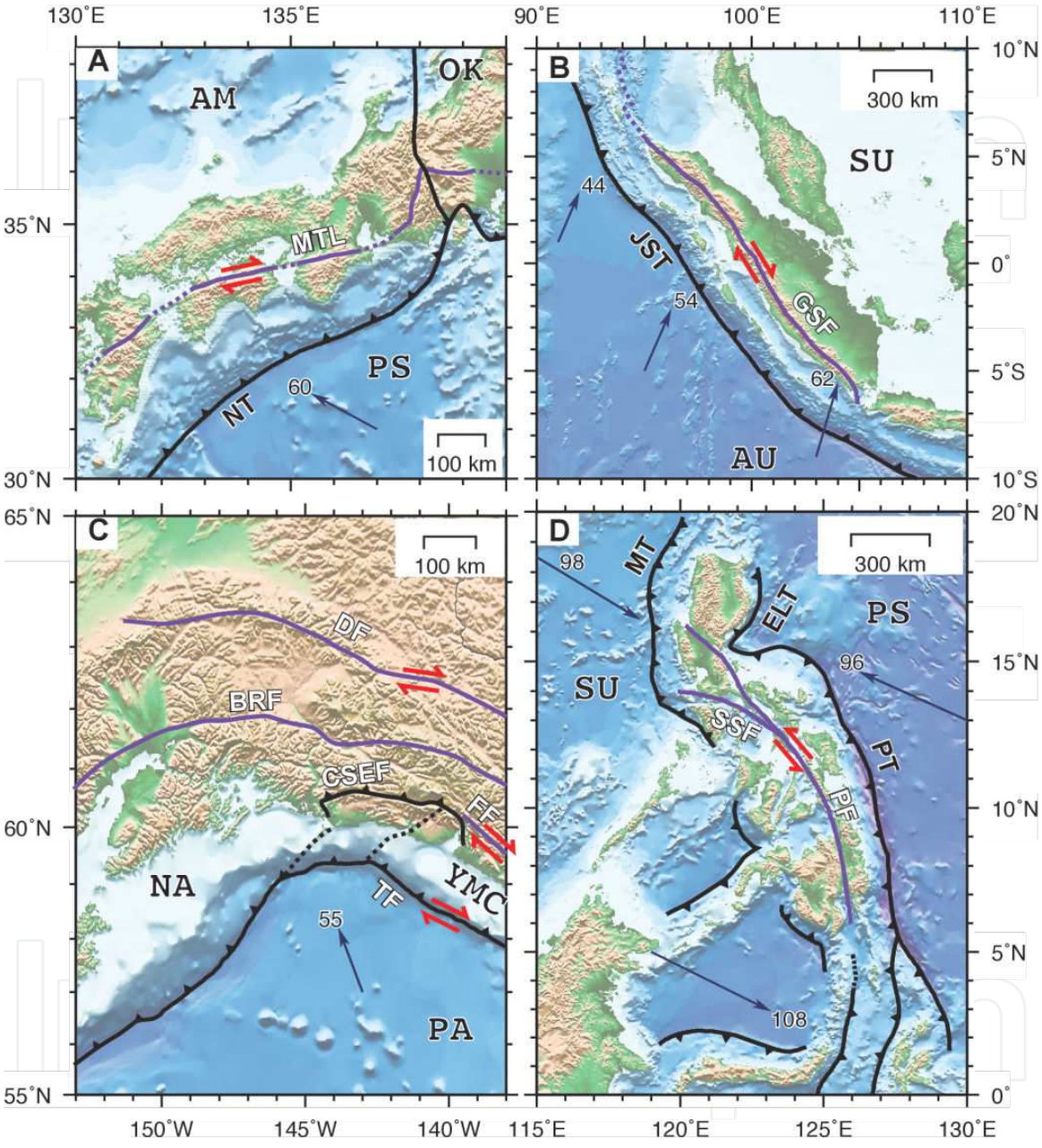

Figure 2. Modern examples of trench-linked strike-slip faults. (A) The Median Tectonic Line (MTL) active fault system in southwestern Japan, related to oblique subduction of the Philippine Sea Plate (PS) along the Nankai Trough (NT). (B) The Great Sumatra Fault system (GSF) along the Java–Sumatra Trench (JST). (C) Strike-slip faults in Alaska. Fault names: DF, Denali; BRF, Boarder Ranges; CSEF, Chugach St. Elias; FF, Fairweather; TF, Transition. (D) The Philippine Fault system (PF). Abbreviations: SSF, Sibuyan Sea Fault; MT, Manila Trench; PT, Philippine Trench; ELT, East Luzon Trough. Plate names: AM, Amur; OK, Okhotsk; PS, Philippine Sea; AU, Australian; SU, Sundaland; NA, North American; PA, Pacific; YMC, Yukutat microcontinent. Black and purple lines are subduction zones and trench-linked strike-slip faults, respectively. All maps were drawn using SRTM and GEBCO with plate boundary data [30]. Blue arrows indicate the direction and velocity of relative plate motion (mm yr^{-1}) based on [31].

These strike-slip faults sometimes separate a narrow sliver plate from the remainder of the over-riding forearc plate. Modern examples include the Median Tectonic Line in Japan, the Sumatra Fault in Indonesia, the Denali Fault in Alaska and the Philippine Fault in Philippine (Figure 2). An ancient example can be observed in the Bering Sea [17]. The strike-slip faults in these settings are typically long (hundreds of kilometers) but occasionally segmented [9].

The Median Tectonic Line (MTL) active fault system is the longest and most active arc-parallel, right-lateral strike-slip fault system in Japan [e.g.18, 19]. The MTL extends over a distance of 500 km and accommodates the trench-parallel component of oblique subduction of the Philippine Sea Plate (Figure 2A).

The Great Sumatra Fault is a right-lateral strike-slip fault more than 1900 km in length (Figure 2B). It is related to the northward subduction of the Australian Plate beneath the Sundaland Plate along the Java–Sumatra Trench (Figure 2B) [20–22].

Strike-slip faulting in Alaska has involved several widely spaced major faults, with an overall seaward migration of activity: the Denali Fault was initiated in the Late Cretaceous or Paleocene and the Fairweather Fault in the Pleistocene (Figure 2C) [23, 24]. These right-lateral strike-slip faults are associated with the Alaskan subduction zone where the Pacific Plate subducts northwestward. Although current strike-slip movement takes place predominantly on the Fairweather Fault, the Denali Fault also shows some Holocene movement.

The Philippine Fault is a left-lateral strike-slip fault sandwiched between the Manila and Philippine trenches [25–27]. It completely traverses the Philippine archipelago and extends for more than 1000 km (Figure 2D). Several strike-slip basins are developed along releasing bends or overstepped faults in this fault zone [28, 29].

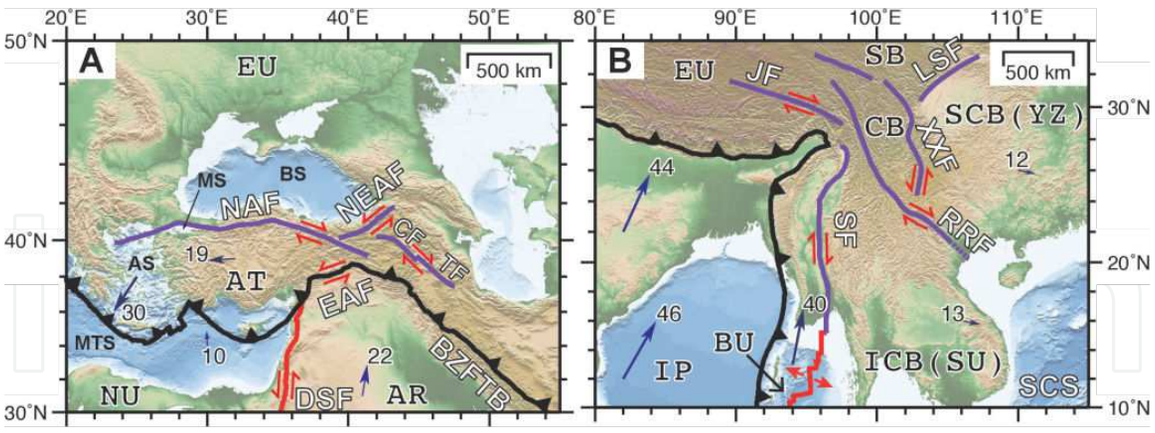

Figure 3. Indent-linked strike-slip fault systems. (A) North Anatolian Fault (NAF) caused by the collision of the Arabian Plate (AR) with the Eurasian Plate (EU). Abbreviations: EAF, East Anatolian Fault; NEAF, Northeast Anatolian Fault; CF, Chalderan Fault; TF, Tabriz Fault; DSF, Dead Sea Fault; BZFTB, Bitlis–Zagros Fold and Thrust Belt; BS, Black Sea; MTS, Mediterranean Sea; MS, Marmara Sea; AS, Aegean Sea. (B) The Red River Fault (RRF) zone, caused by the collision of the Indian Plate (IP) with the Eurasian Plate. Abbreviations: SCB, South China Block; SB, Songpan Block; CB, Chuandian Block; ICB, Indochina Block; SF, Sagaing Fault; JF, Jiali Fault; XXF, Xianshuihe–Xiaojiang Fault; LSF, Longmen Shan Fault. Faults and blocks are based on [33]. Plate names: EU, Eurasian; AR, Arabian; NU, Nubia (Africa); AT, Anatolian; SU, Sundaland; BU, Burma; YZ, Yangtze. Maps were drawn using SRTM and GEBCO with plate boundary data [30]. Black, red, and purple lines are plate convergent margins, plate-boundary transform faults, and indent-linked strike-slip faults, respectively. Blue arrows indicate the direction and velocity of plate motion (mm yr^{-1}) relative to the Eurasian Plate based on [31]

http://dx.doi.org/10.5772/56593

2.2. Continental collision zones

Continental collision can cause crustal shortening and thickening by thrusting and escape or by extruding crustal blocks along conjugate strike-slip faults within the plate. These types of collision-related strike-slip faults between continental blocks are classified as indent-linked strike-slip faults (Figure 1) [9].

Modern examples include several strike-slip faults in Turkey where the Arabian Plate is converging with the Eurasian Plate, and in southern China where the Indian Plate is colliding with the Eurasian Plate (Figure 3). In the latter example, the collision originally formed the left-lateral Red River Fault associated with the southeastward extrusion of the Indochina Block [32]. After the propagation of the indent, the South China Block was extruded along the pre-existing Red River Fault as a block boundary with right-lateral movement.

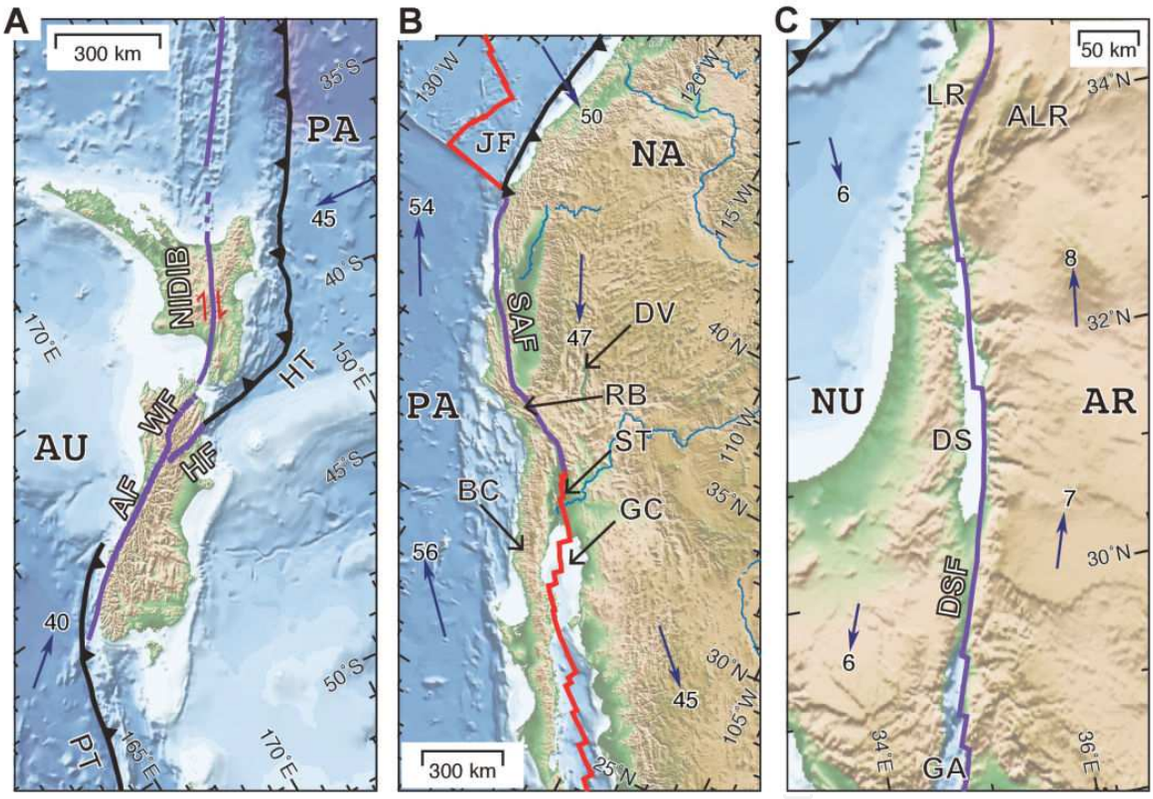

Figure 4. Plate-boundary transform fault systems. (A) Alpine Fault (AF) in New Zealand. Abbreviations: HF, Hope Fault; WF, Wairau Fault; NIDFB, North Island Dextral Fault Belt; HT, Hikurangi Trough; PT, Puysegur Trench. Faults are from [34] and [35]. (B) San Andreas Fault systems (SAF) in North America. Abbreviations: DV, Death Valley; RB, Ridge Basin; ST, Salton Trough; GC, Gulf of California; BC, Baja California Peninsula. (C) Dead Sea Fault systems. Abbreviations: DS, Dead Sea; GA, Gulf of Aqaba; LR, Lebanon Range; ALR, Anti-Lebanon Range. Plate names: PA, Pacific; AU, Australian; NA, North American; JF, Juan de Fuca; AR, Arabian; NU, Nubian (African). All maps were drawn by using SRTM and GEBCO with plate boundary data [30]. Black, red, and purple lines are subduction zones, oceanic spreading ridges, and plate-boundary transform faults, respectively. Blue arrows indicate the direction and velocity of relative plate motion (mm yr^{-1}) based on [31]

2.3. Plate-boundary transform zones

Plate-boundary transform faults develop between two plates rotating around the poles that define the relative motion between them [9]. The San Andreas Fault, Dead Sea Fault, Alpine Fault (New Zealand), and the northern and southern margins of the Caribbean Plate are modern examples of this type (Figure 4).

3. Strike-slip basins

Strike-slip faults can accommodate localized compression or extension at continental margins, in island arcs, and also within continents. Sedimentary basins commonly develop where the fault kinematics are divergent with respect to the plate vector along strike-slip faults. Since the 1980s, various classifications of strike-slip basins have been formulated [4, 11, 36–40]. Common characteristics of strike-slip basins [4, 39] include: (1) elongated geometry, (2) asymmetry of both sediment thickness and facies pattern, (3) dominance of axial infilling, (4) coarser-grained marginal facies along the active master fault, (5) finer-grained main facies, (6) depocenter migration opposite to the direction of axial sediment transport, (7) very thick strata relative to the burial depth, (8) high sedimentation rate, (9) abrupt lateral and vertical facies changes and unconformities, (10) compositional changes that reflect horizontal movement of the provenance, (11) abundant syn-sedimentary slumping and deformation, and (12) rapid subsidence in the initial stage of basin formation.

There are many strike-slip basins along plate convergent margins (Figure 5 and Table 1). Here I classify strike-slip basins into four types, discussed in turn below.

	Indent-linked strike-slip faults	**Trench-linked strike-slip faults**	**Plate boundary transform faults**
Fault-bend basin	Vienna Basin[1] Marmara Sea[2]	Izumi Group*[3] St. George Basin*[4] Suwa Lake[5]	Ridge Basin*[6] Death Valley[7]
Stepover basin	Thai Basin[8]	Matsuyama Plain[9] Salan Grande Basin[10]	Dead Sea Basin[11] Cayman Trough[12] Cariaco Basin[13] Salton Trough[14]
Fault-termination basin	Yinggehai Basin[15] Malay Basin[16]	Beppu Bay[17]	Gulf of California[18]
Transpressional basin		Aceh Basin[19] Tokushima Plain[20]	

Table 1. Modern and ancient (*) examples of strike-slip basins according to the types of strike-slip faults. Numbers correspond to those in Figure 5

http://dx.doi.org/10.5772/56593

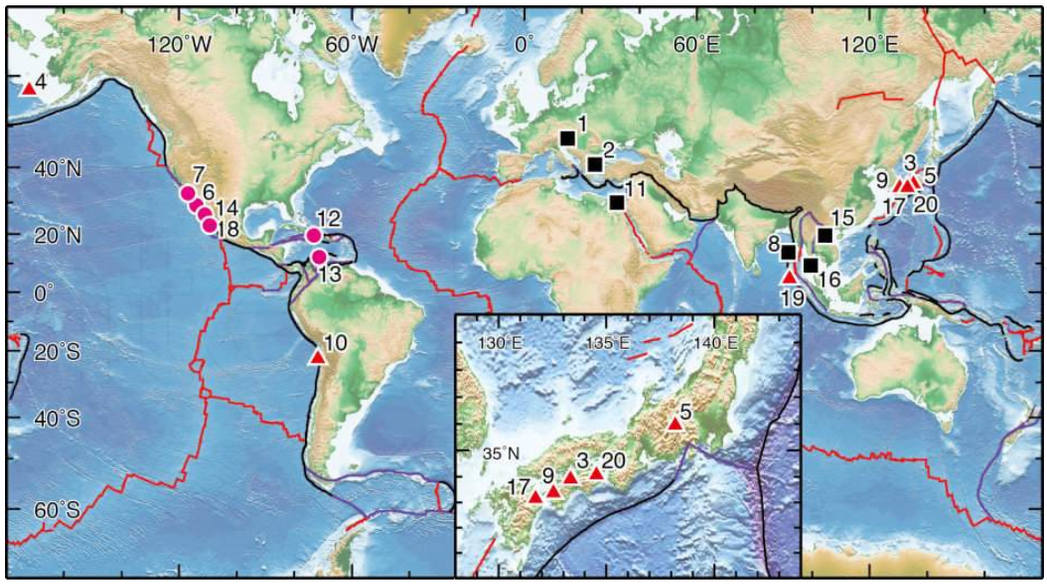

Figure 5. Strike-slip basins at plate convergent margins. Red triangles, trench-linked; black squares, indent-linked; purple circles, plate-boundary transform faults. Numbers correspond to those in Table 1

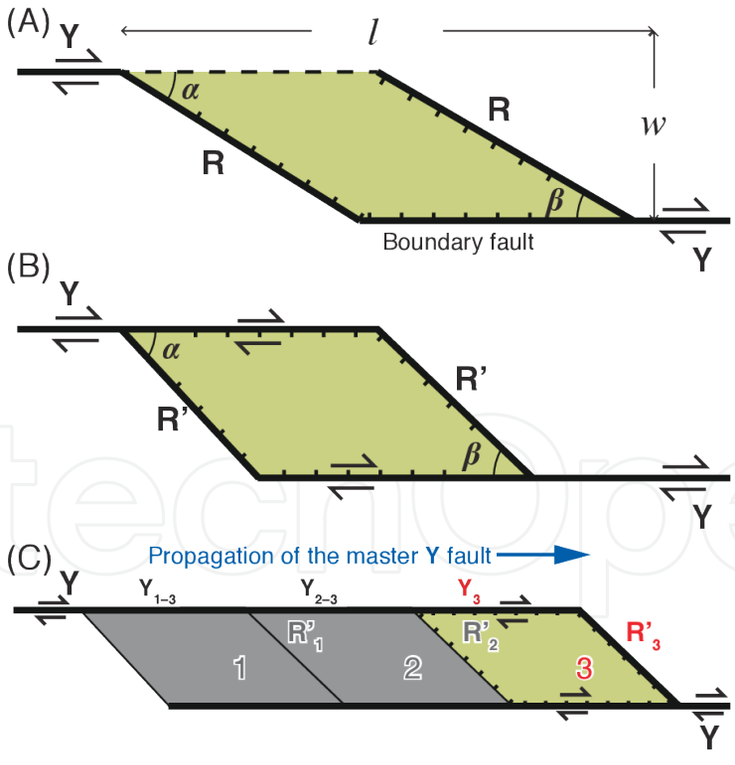

Figure 6. Geometrical models of (A) a spindle-shaped fault-bend basin and (B) a rhomb-shaped stepover strike-slip basin. Colored areas indicate subsiding basins. (C) Multistage evolution of stepover basins. As a result of step-wise propagation of one of the master faults, a new basin (3) is created, but the pre-existing basins 1 and 2 become inactive, resulting in a long (high *l*/*w* ratio) strike-slip basin with progressive depocenter migration. Diagrams are modified from [42]

3.1. Fault-bend basins

Fault-bend basins result from vertical displacement of normal faults in front of releasing bends corresponding to gentle transverse **R** (synthetic Riedel) faults connected to stepped master **Y** (principal displacement) faults (Figures 1 and 6A). The basin geometry is generally spindle-shaped or lazy-Z-shaped in plan view [38]. This type is considered to represent an early stage of the evolution of a pull-apart basin [12].

3.2. Stepover basins

As the master faults continue to propagate, they overlap and pull the crustal blocks farther apart, with lengthening geometries that gradually change from lazy-Z-shaped fault-bend basins to rhomboid-shaped stepover basins (Figure 6B). The basins subside by extension along strike-slip fault systems where the sense of *en échelon* segment stepping coincides with the sense of the slip (i.e., right-stepping faults have dextral displacement). The term 'pull-apart basin' was originally introduced to explain a depression in the Death Valley whose sides were pulled apart along releasing bends or oversteps of faults [41]. According to the pull-apart mechanism, two sides of the basin are bounded by faults with primarily horizontal displacement, and the other two sides are bounded by listric or transverse faults.

Stepover basins generally maintain their length/width ratio [2], as expressed by the following relationship between the length (l) and width (w) of a pull-apart basin based on the dimensions of natural pull-apart basins (Figure 6):

$$\log l = c_1 \log w + \log c \tag{1}$$

The best fitting constants have been found to be $c_1 = 1.0$ and $c_2 = 3.2$, which yield $l/w \approx 3.2$ with a 95% confidence interval about the ratio of $2.4 < l / w < 4.3$.

In sandbox experiments [42], a spindle-shaped basin appears in the first stage of basin evolution and is bounded by master **Y** faults and their synthetic Riedel (**R**) faults. Subsequently, antithetic Riedel (**R'**) faults replace **R** faults, leading to a rhomb-shaped basin. The l/w ratio depends on the angles α and β (Figure 6):

$$l / w = 1 / \tan\alpha + 1 / \tan\beta \tag{2}$$

The mean angle between **R** and **Y** faults in the experiments is $a = \beta = 30^{o}$; that is, l/w=3.5. This value is consistent with those of natural basins.

As overlapped offsets of the master strike-slip faults propagate, basins elongate and finally become long pull-apart basins. The Dead Sea Basin, with a length of 132 km and a width of 18 km (l/w=7.2), is considered to have been formed by the coalescence of three successive and adjacent sedimentary basins whose depocenters migrated northward with time [43]. Although each sub-basin has a l/w ratio typical of a pull-apart basin (2.4, 3.3, and 2.6 from south to north),

http://dx.doi.org/10.5772/56593

propagation of the master fault, accompanied by the creation of a new stepover basin, has resulted in the basins high *l*/*w* ratio (Figure 6C) [42].

Very high *l*/*w* ratios can also result from continuous transtension leading to extreme thinning of the crust and rupture. This process induces magmatic activity, high heat flow, and then the generation of new oceanic crust that may be younger than the overlying sedimentary succession (e.g., the Cayman Trough or the Gulf of California).

3.3. Fault-termination basins

Fault-termination basins are developed in transtensional stress domains at the ends of strike-slip faults where normal or oblique slip faults diffuse or splay off to terminate the deformation field [44]. If a part of a crustal block undergoes translation within the block, it results in shortening/uplift at one end and extension/subsidence at the other (Figure 7). Basins formed by such subsidence are referred to as fault-termination basins or transtensional fault-termination basins [44].

Modern examples include the Yinggehai Basin (Song Hong Basin) along the Red River Fault zone [45], the Malay and Pattani basins in the Gulf of Thailand [46], several segmented basins in the Gulf of California [44, 47], the northern Aegean Sea [48, 49], and Beppu Bay along the Median Tectonic Line (Figure 5 and Table 1) [50].

3.4. Transpressional basins

Transpressional basins tend to develop along oblique convergent margins whose subsidence results from flexural loading of the hanging-wall crust, similar to foreland basins adjacent to uplifted blocks [52–54]. Such basins are usually long, narrow structural depressions that lie parallel to the master faults.

The Sumatra forearc basins are modern examples of this type. Uplift of outer arc highs bounded by trench-linked strike-slip faults may cause flexural subsidence on the forearc side and generate elongate wedge-shaped sedimentary basins.

4. Examples of strike-slip basins

The wide variability of strike-slip faults makes it difficult to develop a simple model of the formation of strike-slip basins and their sedimentary facies. Although the geometries of such basins depend on the amount of fault displacement, the angle and distance between overstepped faults, and the depth of detachment of the faults, the basins are generally elongate, narrow, and deep. Several representative examples of the strike-slip basins described in this section show a range of basin evolutionary paths and filling processes.

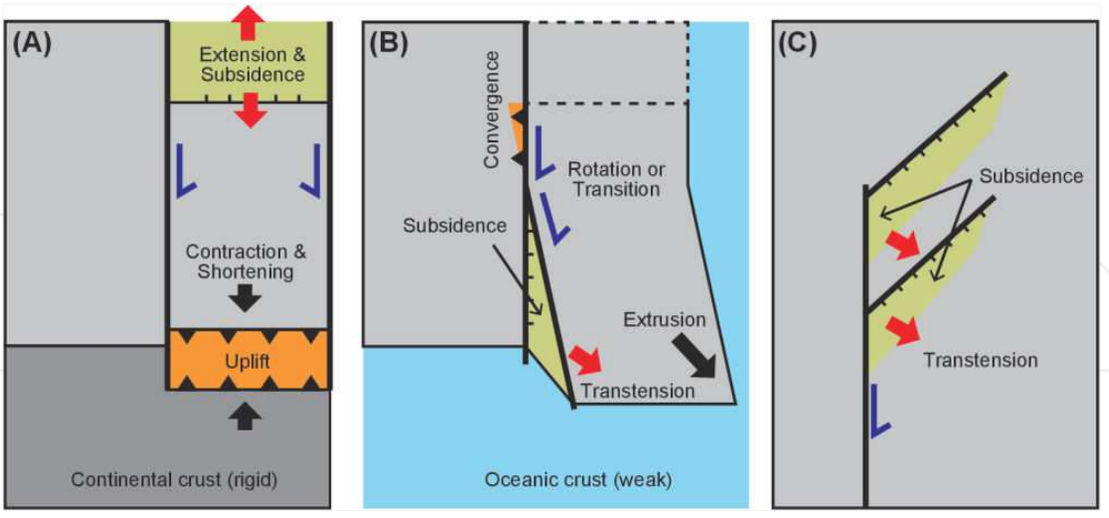

Figure 7. Typical geometry of termination areas of strike-slip faults. (A) If the block collides with a rigid continental crust, it shortens and is uplifted, accompanied by thrusts. At the opposite side to the uplift, upper crust is mechanically pulled away, leading to subsidence. (B) If the block extrudes with a rotational component into a weak oceanic crust (a transtensional setting), a sedimentary basin forms at the end of the strike-slip fault. Examples include the Yinggehai Basin, which is related to the extrusion of the Indochina Block, and the Gulf of California, which is related to the transtensional movement of the Baja California Peninsula. (C) The strike-slip fault diffuses its displacement through splayed extensional normal faults at its end [44]. An example is the Cerdanya clastic basin formed by late Miocene normal faulting at the termination of the La Tet strike-slip fault, Spain [51].

4.1. Fault-bend basin: The Ridge Basin

4.1.1. Geology

The Ridge Basin, which is one of the best-studied examples of a strike-slip basin [37, 55], is situated along the San Andreas Fault, a right-lateral plate-boundary transform fault between the Pacific and the North American plates, and along the San Gabriel Fault, a major strand of the San Andreas Fault (Figure 4B).

The San Gabriel Fault is a listric, ESE-dipping, oblique-slip fault rather than a subvertical, strike-slip fault [56]. The Ridge Basin is a type of fault-bend basin developed in front of a releasing bend on the San Gabriel Fault, along which the upper crust stretched and subsided to form a space in which sediments could be accommodated. The bottom of the basin is bounded by the subhorizontal San Gabriel Fault at a depth of ~4 km.

The basin originated in the late Miocene as a narrow depression within the broad San Andreas transform belt in southern California. The basin has a length of 45 km and a width of 15 km; the length/width ratio of 3 is a typical value for pull-apart basins [2]. The strata are exposed as a northwest-dipping homoclinal sequence that becomes younger to the northwest. The exposed sediment thickness reaches ~14 km, somewhat larger than the basin depth (~4 km) [56].

http://dx.doi.org/10.5772/56593

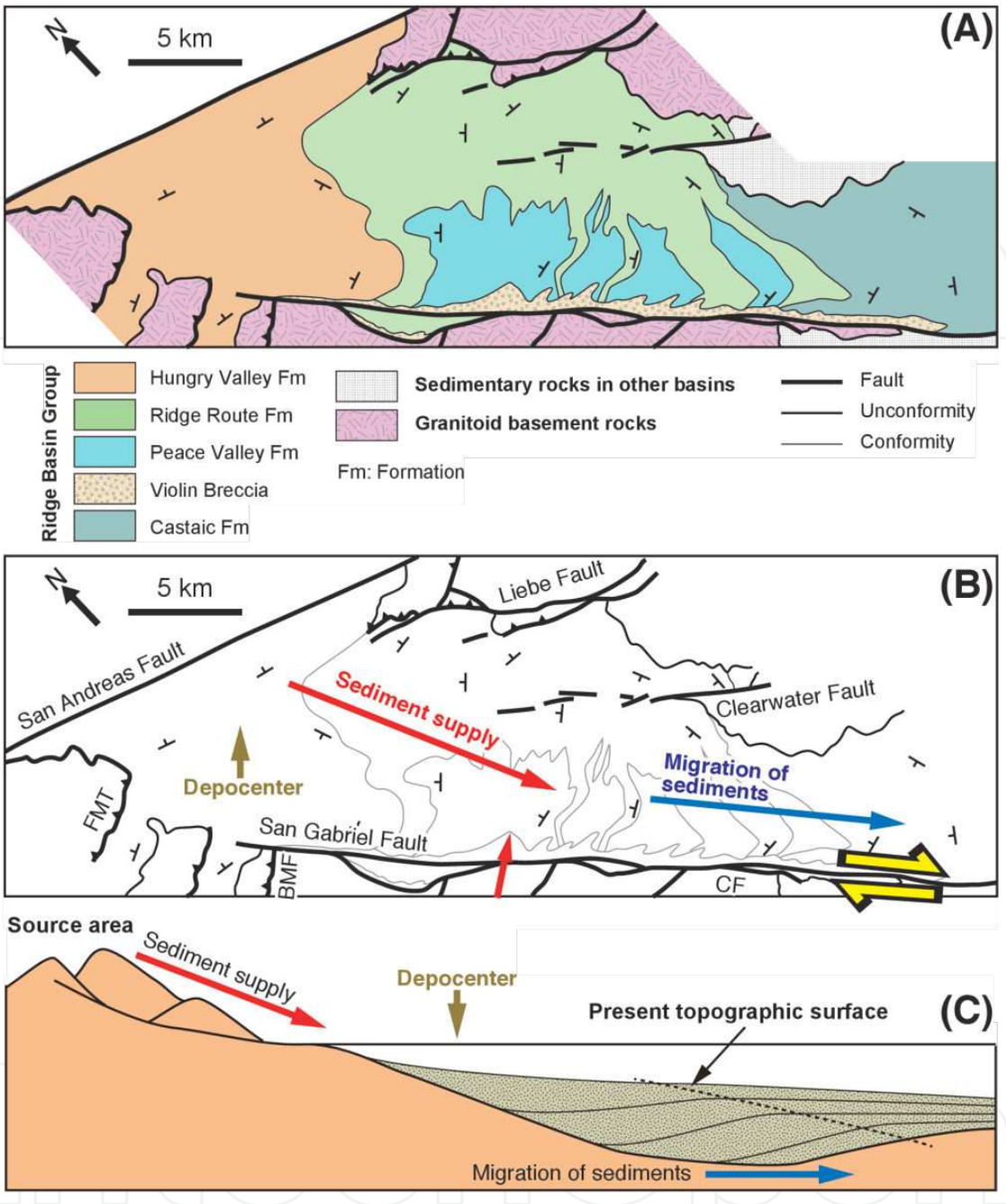

Figure 8. (A) Simplified geological map showing formations in the Ridge Basin [58]. (B) Conceptual basin-filling process for the Ridge Basin [8]. Abbreviations: FMT, Frazier Mountain Thrusts; BMF, Bear Mountain Fault; CF, Canton Fault. (C) Cross-sectional profiles showing continuous axial sediment supply and migration of sediments with relatively fixed depocenters [61]

4.1.2. Basin filling processes

The strata within the Ridge Basin are assigned to the Ridge Basin Group, which includes five formations: Castaic, Peace Valley, Violin Breccia, Ridge Route, and Hungry Valley (Figure 8A). Sedimentation began in the late Miocene (ca. 11 Ma) with deposition of the marine Castaic

Formation. The younger Castaic Formation is interfingered with the older Violin Breccia, which consists of conglomerates adjacent to the San Gabriel Fault scarp [57].

The main part of the Ridge Basin Group consists of the Peace Valley and Ridge Route formations. The Peace Valley Formation consists mainly of sandstone and mudstone of lacustrine, fluvial, deltaic, and alluvial facies, accompanied by minor carbonaceous deposits. The Ridge Route Formation, which crops out in the northeastern part of the Basin, is composed of alluvial sandstone and conglomerate, and is interfingered with the Peace Valley Formation. Both the Peace Valley and Ridge Route formations are interfingered southwestward into the Violin Breccia. The uppermost unit of the Ridge Basin, the Hungry Valley Formation, conformably overlies the Peace Valley and Ridge Route formations. The deposition of this formation, including alluvial conglomerate, sandstone, and mudstone, ended at ca. 4 Ma.

The Ridge Basin Group presents a 14-km-thick stratigraphic section of gently (20–25°) northwest-dipping beds; it shows the dominance of axial sediment supply and migration of the deposits by dextral movement of the San Gabriel Fault (Figure 8B). The releasing bend may have a paired restraining bend on the northwestern side of the fault. Within the restraining bend, highlands were formed, which in turn provided sediment to be transported into the basin. Most of the sediment filling the basin was carried by rivers draining source areas located to the northeast. The sediments forming the Ridge Basin Group were deposited at a rate of about 2 m kyr^{-1}.

The right-lateral displacement of the San Gabriel Fault carried the basin, together with the sediments, southeastward, resulting in a northwestward migration of the depocenter and successively younger beds onlapping onto the basin floor (Figure 8C) [58, 59]. Nearly constant values of vitrinite reflectance data (Ro = 0.5) throughout the group [60] support the continuous removal of sedimentary strata deposited in a relatively fixed depocenter and transported to the southeast along the San Gabriel Fault. More than 45 km of lateral displacement is estimated, based on the distribution of the Violin Breccia. This displacement, and basin migration, ended in the early Pliocene.

4.2. Stepover basin: The Dead Sea Basin

4.2.1. Geology

The Dead Sea Fault system is located along a plate-boundary transform zone that separates the Arabian Plate from the African Plate (Figures 4C and 9) [12]. Movement along the Dead Sea Fault commenced in the Miocene in response to the opening of the Red Sea. The very low rate of relative plate motion between Arabia and Africa (6–8 mm yr^{-1}) has yielded only 30 km of displacement during the past 5 Myr, and about 105 km of total offset during the past 18 Myr.

The Dead Sea Fault system includes both transpressional and transtensional domains (Figure 9). Several strike-slip basins are developed along the steps of segmented faults in the transtensional domain, while the Lebanon and Anti-Lebanon ranges have been uplifted in the transpressional domain related to the restraining bend. The Dead Sea Basin is the largest strike-

http://dx.doi.org/10.5772/56593

slip basin in the system, and is partly overlain by a deep hypersaline lake located at Earth's lowest continental elevation (418 m below sea level at the lake surface) [43, 62–64].

The Dead Sea Basin is 132 km long and 7–18 km wide, yielding a high length/width ratio (> 7). The basin is segmented into sequential sub-basins by deep transverse normal faults rather than by listric faults. The length of the basin is greater than the total offset length (~105 km) of the fault system, which is atypical of pull-apart basins [65].

The basin has a cross-sectional asymmetry, with a steep eastern slope and a gentle western slope. Seismic refraction and gravity data indicate that the southern Dead Sea Basin is unusually deep, containing about 14 km of sedimentary fill [66]. Geophysical data suggest that the deep basin is probably bordered on all sides by vertical faults that cut deep into the basement [67]. The thick sediment accumulation yields a large negative Bouguer gravity anomaly (lower than –100 mGal) [64]. Given the depth of the basin, ductile deformation in the lower crust would be expected; however, the present-day heat flow in the Dead Sea Basin is low (~40 mW m^{-2}) [68], suggesting that the lower crust may still be cool and brittle, and that the Moho is not elevated beneath the basin. These inferences are consistent with seismic activity at depths of 20–32 km.

The Dead Sea Basin has traditionally been considered a classic example of a stepover basin [2], but other interpretations have been proposed, including propagating basins [67], stretching basins [64], and sequential basins [63]. The sequential basin model, in which several active sub-basins are delimited by boundary master faults and transverse faults, and simultaneously

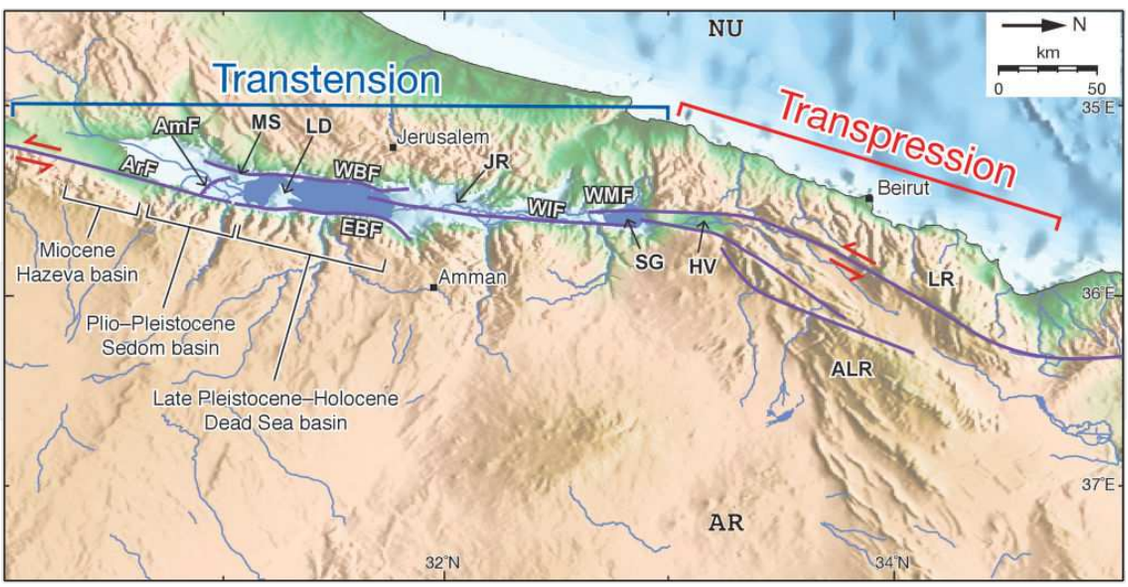

Figure 9. The Dead Sea Basin developed in a transtensional domain of the Dead Sea Fault system. On the northern side of the basin, the Lebanon and Anti-Lebanon ranges were uplifted in a transpressional domain. The locations of faults are taken from [12]. Abbreviations: AmF, Amaziyahu Fault; ArF, Arava Fault; WIF, Western Intrabasinal Fault; EBF, Eastern Boundary Fault; WBF, Western Boundary Fault; MS, Mount Sedom; LD, Lisan Peninsula; LR, Lebanon Range; ALR, Anti-Lebanon Range; JR, Jordan River; SG, Sea of Galilee [69]; HV, Hula Valley [70]. Plate names: AR, Arabian; NU, Nubian (African).

become larger and deeper as the master faults propagate, could explain why the Dead Sea Basin is longer than the total amount of slip along the Dead Sea Fault.

4.2.2. Basin-filling processes

The depositional environments of the Dead Sea Basin are affected by the arid climatic conditions, with the area having an average annual rainfall of 50–75 mm. The modern sediments are transported to the basin mainly from the north by the Jordan River and from other directions by marginal tributaries. The mean annual discharges from the north, east, west, and south are 1100, 203, 4–5, and 4 mm, respectively [71].

In the middle to late Miocene, fluvial clastics of the Hazeva Formation were deposited in the southern sector of the basin (Figure 9). The formation consists of fluvial sandstones and conglomerates, including pre-Cretaceous components, transported from distant sources south and southeast of the Dead Sea Basin [43, 64]. During the Pliocene, the evaporitic Sedom Formation accumulated in estuarine–lagoonal environments in the Dead Sea basin; the formation consists mostly of lacustrine salts, gypsum, and carbonates interbedded with some clastics, and is found in the central sector of the basin. The 2–3 km thickness of this evaporitic formation may have formed in < 1 Myr; therefore, the sedimentation rate was probably higher than 2 m kyr^{-1}.

In the Pleistocene and Holocene, fluvial and lacustrine deposits, alternating with evaporites and locally sourced clastics, accumulated in lakes that post-date the formation of the Sedom lagoon. The Amora, Lisan, and younger formations consist of laminated evaporitic (gypsum) and aragonite sediments that continue to accumulate in the modern Dead Sea in the northern sector of the basin. The average sedimentation rate in this stage reached 1–1.5 m kyr^{-1} [64]. On the whole, the depocenters have migrated northward since the Miocene.

The margins of the Dead Sea are dominated by alluvial fans. The modern basin margin environments consist of (1) talus slopes, (2) incised and confined stream channels, and (3) coarse-grained and relatively high-gradient alluvial fans. In contrast, sediments in the offshore environment are composed of thick sequences of evaporitic salt intercalated with thin beds of laminated aragonite and detrital silt [72].

4.3. Fault-termination basin: The Yinggehai Basin

4.3.1. Geology

The Yinggehai Basin (Song Hong Basin) is an example of a fault-termination basin, and is situated at the southeastern end of the Red River Fault zone (RRFZ) [73, 74]. The RRFZ, extending for some 1000 km, separates the South China Block to the north from the Indochina Block to the south (Figure 10), and is considered to be related to the continental collision between the Indian and Eurasian plates [e.g., 75]. The formation of the Yinggehai Basin was controlled by the successive clockwise extrusions of the Indochina Block and the South China Block.

http://dx.doi.org/10.5772/56593

The RRFZ was a sinistral strike-slip fault in the first stage of its evolution (34–17 Ma), associated with ductile deformation [76] and the creation of an unconformity in the Gulf of Tonkin (the offshore part of the Hanoi depression [77]). After a quiescent stage from 17 to 5 Ma, due to a slowdown in the clockwise rotation of the Indochina Block [78], the movement along the RRFZ became dextral [45, 79, 80]. The right-lateral shearing is indicated by geomorphic fault traces and large river offsets [81–83], as well as GPS observations [80]. This change from a sinistral to a dextral sense of movement supports the basic tenets of the two-phase extrusion model; namely, the early, collision-driven escape of Indochina towards the SE, and the subsequent change to accommodate the present-day escape of Tibet and South China [78, 84, 85].

The Yinggehai Basin, situated in the offshore extension of the RRFZ, is 500 km long and 50–60 km wide ($l/w \approx 10$); it is oriented SE–NW and is located offshore between Hainan Island to the east and the Indosinian Peninsula to the west [73]. The basin formed originally as a sinistral strike-slip basin [77, 86], but developed into a dextral strike-slip basin after the change in the sense of fault displacement of the RRFZ [87, 88]. The basin subsided by simple shear on low-angle, detached normal faults of the upper crust and by pure shear of the lower crust [45, 87].

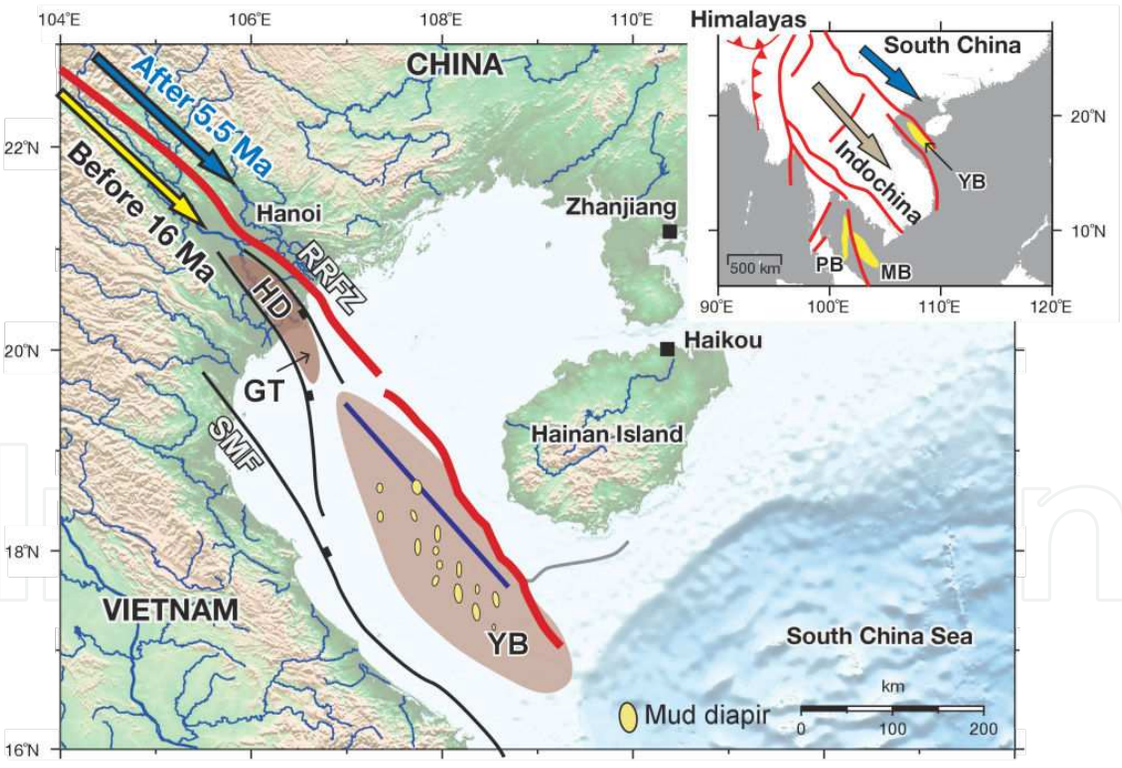

Figure 10. Geological setting of the Red River Fault zone (RRFZ) and the Yinggehai Basin. The RRFZ was originally a left-lateral strike-slip fault caused by the southeastern extrusion of the Indochina Block. The sense of displacement changed to right-lateral in response to the southeastward extrusion of the South China Block. Abbreviations: SMF, Song Ma Fault; HD, Hanoi Depression; GT, Gulf of Tonkin; YB, Yinggehai Basin; MB, Malay Basin; PB, Pattani Basin. The thick blue line marks the cross-sectional profile displayed in Figure 11. Modified from [80, 89, 90].

4.3.2. Basin-filling processes

The Yinggehai Basin is filled with 10–17-km-thick clastic deposits [45]. Basin sedimentation began in the late Eocene [45, 88]. During the Oligocene (> 21 Ma), clockwise rotation of the Indochina Block induced sinistral slip along the RRFZ and the basin rapidly subsided and started to fill. The depocenter was situated in the southern part of the basin during this syn-rift stage (Figure 11) [45, 91]. During the quiescent post-rift stage of the RRFZ, the rate of basin subsidence accordingly decreased and the depocenter gradually migrated northwestward [45]. The reactivation of the RRFZ with dextral movement triggered rapid subsidence [80] and enhanced the input of sediment [45]. The depocenter migrated from the center to the south-eastern end of the basin (Figure 11).

The infill of the Yinggehai Basin varies from alluvial, fluvial, and lacustrine deposits (before 21 Ma, the syn-rift stage) to marine sediments (after 21 Ma, the post-rift stage) [80]. Almost all the sediments in the basin are considered to have been derived from the Himalayas through the Red River drainage network [92]. Large mountain belts with high rates of sediment yield and along-fault transport networks were able to effectively supply huge volumes of detritus into the basin. Thick sediments and high sedimentation rates resulted in an over-pressured condition leading to mud diapirism [73], and also to depressed surface heat flow (~80 mW m^{-2}) [93]. The orientations of mud diapirs in the basin (Figure 13) indicate E–W extension related to right-lateral motion of the northeastern bounding fault [89, 90].

The Pattani and Malay basins in the Gulf of Thailand (inset map in Figure 10) are also considered to be fault-termination basins related to the continental collision of the Indian Plate [94, 95, 96]. Sediment supply into the basins is dominated by rivers flowing along the strike-slip faults [97, 98]. The Pattani and Malay basins contain thicknesses of sediment of more than 8 and 14 km, respectively. The subsidence of the basins was controlled at first by tectonic depression related to strike-slip deformation and then by thermal subsidence due to high surface heat flow (100–110 mW m^{-2}) [46, 99–101].

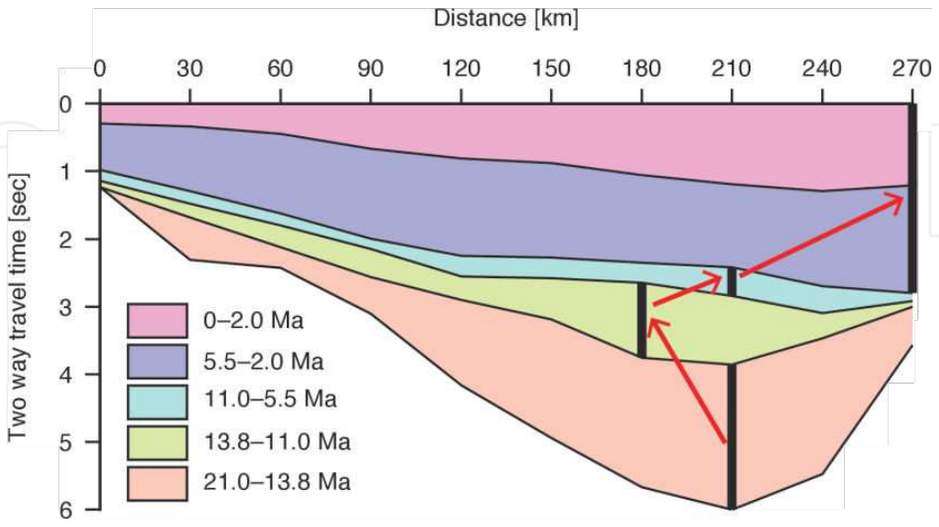

Figure 11. Sediment thickness in the Yinggehai Basin along the profile line shown in Figure 10. Red arrows suggest depocenter migration based on the thickest parts of the sediments deposited in each period (shown by solid vertical lines). Modified from [45].

http://dx.doi.org/10.5772/56593

4.4. Transpressional basin: The Aceh Basin

4.4.1. Geology

Sumatra is a classic example of slip partitioning due to an obliquely subducting plate [14]. The Indian and Australian plates are subducting beneath the Sundaland Plate in southeastern Asia along the Java–Sumatra Trench (Figure 2), where oblique subduction is accompanied by trench-parallel forearc translation [21]. The subduction thrust and the trench-parallel strike-slip fault (Great Sumatra Fault) isolate a wedge of forearc in the form of a sliver plate (the Burma Plate). The Great Sumatra Fault extends along the entire length of Sumatra Island (>1900 km) [22] and finally joins the West Andaman Fault (WAF), which constitutes a series of transform faults and spreading centers in the Andaman Sea [102]. In the forearc sliver, outer-arc uplift related to development of the accretionary prisms occurs on the trenchward side, and forearc basins (the Aceh and Simeulue basins) are developed on the landward side.

The Aceh Basin (Figures 12 and 13) is a wedge-shaped forearc basin with a long (> 200 km) and narrow (< 50 km) geometry ($l/w > 4$) bounded by the West Andaman Fault, a trench-linked strike-slip fault obliquely crossing the northward extension of the Great Sumatra Fault [103–

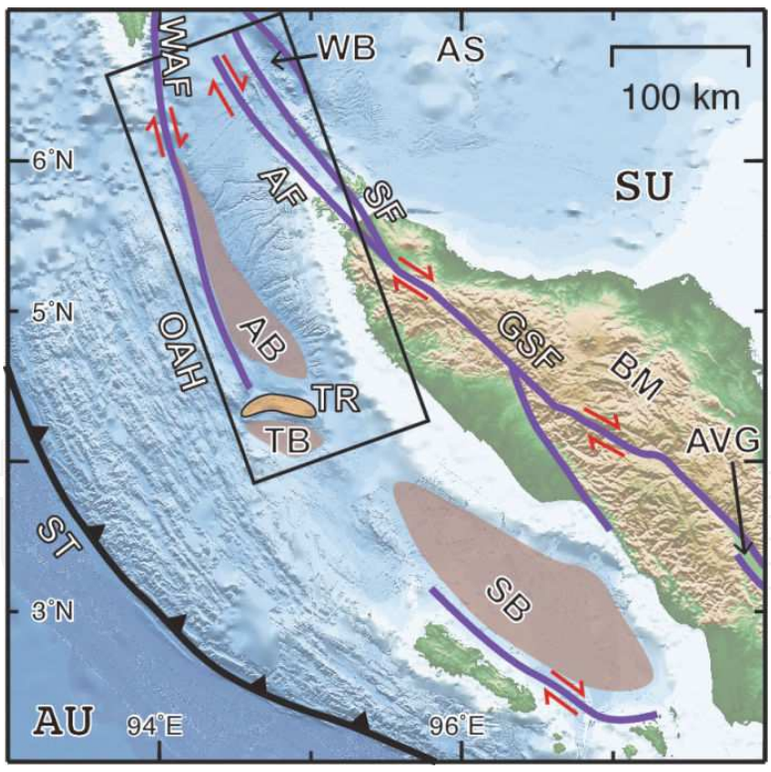

Figure 12. Physiographic map of the Sumatra region. Purple lines are strike-slip faults. Abbreviations: GSF, Great Sumatra Fault; AF, Aceh Fault; SF, Simeulue Fault; WAF, West Andaman Fault; AB, Aceh Basin; TR, Tuba Ridge; TB, Tuba Basin; SM, Simeulue Basin; WB, Weh Basin; BM, Barisan Mountain Range; AVG, Alas Valley Graben; OAH, outer-arc high; ST, Sumatra Trench; AS, Andaman Sea. The Weh Basin and Alas Valley graben are considered to be stepover pull-apart basins [22, 102]. The enclosed area is shown in Figure 13. Bathymetry is based on using SRTM and GEBCO with the data recently collected by [108–110].

106]. The bounding fault is a right-lateral transpressional fault with accompanying topographic highs of *en échelon* anticlines on the western margin and compressional ridges of Tuba Ridge on the southern margin (Figure 13). The transpressional uplift generating the outer-arc high by a thickening crustal block may be resulting in subsidence opposite to the high. This type of sedimentation is similar to that of foreland basins, where depressions are caused by the overburden pressure of the thrusted crust. Rifting and basin formation started in Sumatra during the Paleogene [107].

4.4.2. Basin-filling processes

The deposits in the basin are thickest along the boundary fault between the basin and the outer-arc high, and gradually thin with increasing distance from the faults (Figure 14B and C). Regarding the recent deposits, represented by seismic units 3 and 4 (Figure 14), unit 3 sediments in the southern part are thicker than those in the northern part, but unit 4 sediments are thicker in the northern part. Therefore, the main depocenter is considered to have migrated from the south (unit 3) to the north (unit 4). This interpretation is supported by seismic profiles of [106], who noted that the southern part of the Aceh Basin is raised above the northern part.

Most of the sediments are considered to have been supplied from Sumatra Island through small submarine channels (Figure 13). However, little is known about axial sediment redistribution within the basin.

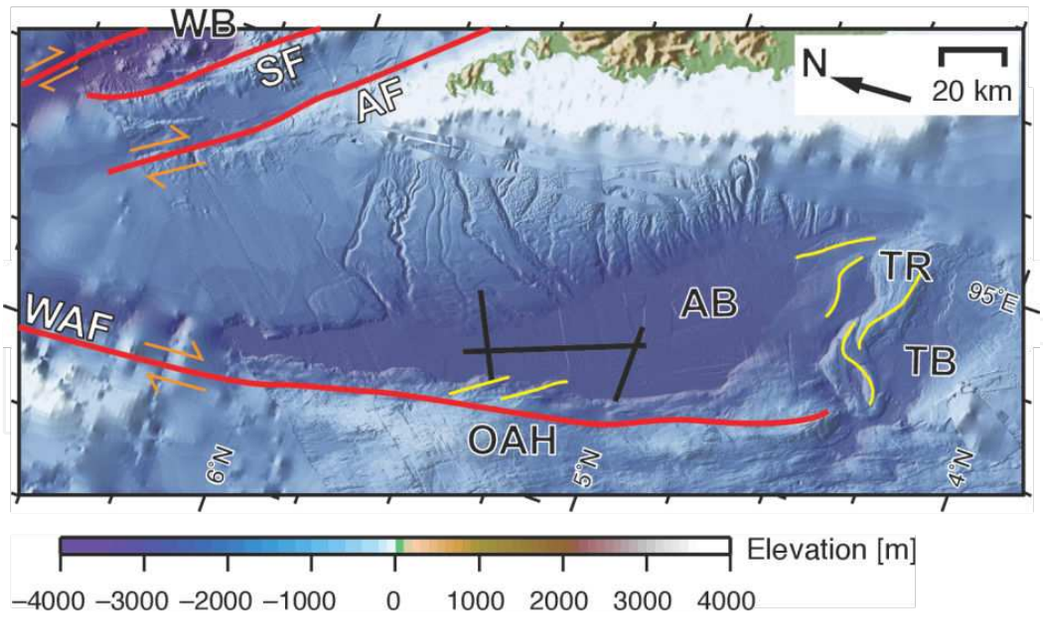

Figure 13. Detailed bathymetry around the Aceh Basin. Red and yellow lines are strike-slip faults and axes of anticlines [105], respectively. Thick solid lines in the Aceh Basin mark cross-sectional profiles shown in Figure 14. Abbreviations are the same as for Figure 12. Bathymetry is based on using SRTM and GEBCO with the data recently collected by [108–110].

http://dx.doi.org/10.5772/56593

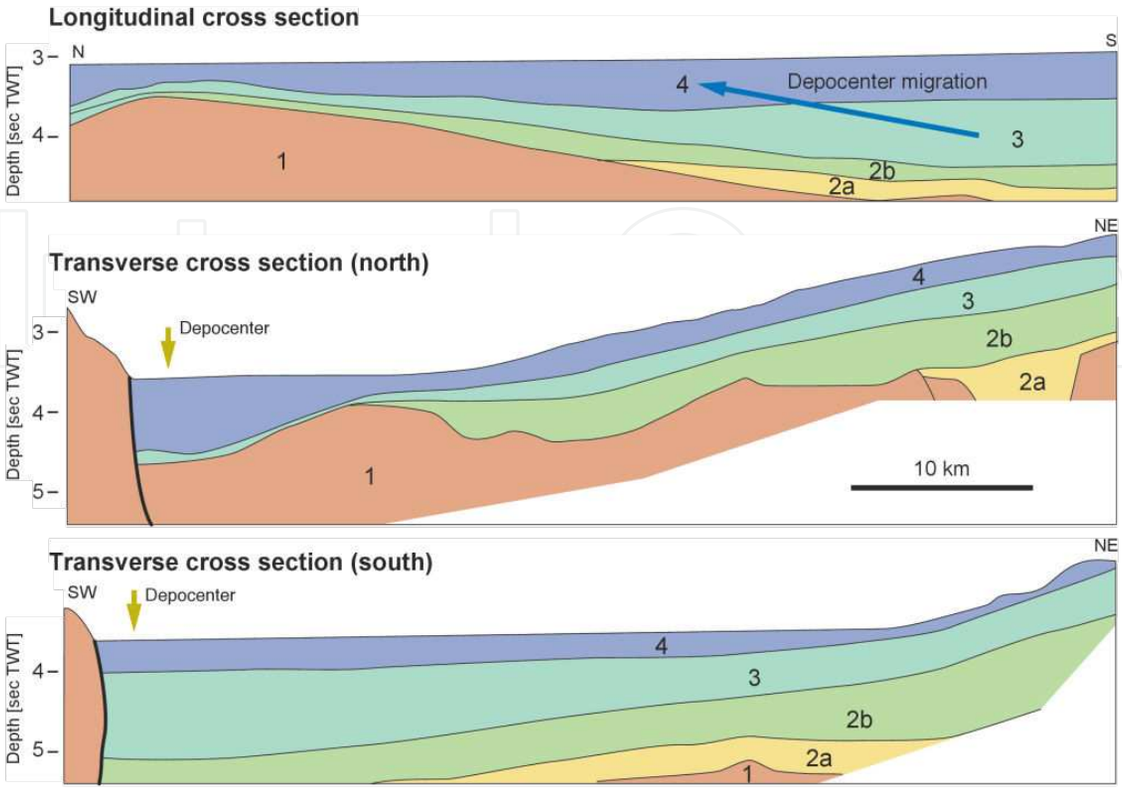

Figure 14. Cross-sectional profiles of the Aceh Basin. The uppermost seismic unit 4 was deposited predominantly in the northern part of the basin, suggesting a northward migration of the depocenter. Modified from [103]

5. Summary

This preliminary review has introduced some of the representative strike-slip basins at convergent margins from the viewpoints of basin formation and filling processes. Because strike-slip basins present a wide range of formational processes and sedimentary facies, it is difficult to establish a simple model of their evolution. To understand both modern and ancient strike-slip basins, the following factors need to be considered:

- Tectonic setting: plate boundary between continental plate or island arc microplate and subducting oceanic plates, collision between continents, within-plate
- Local stress field: compression, transpression, pure strike-slip, transtension, extension
- Fault configuration: existence of releasing or restraining bend, directions and dips of boundary and transverse faults, offset length of overstepped master faults
- Basin geometry: length, width, depth
- Thermodynamic condition: heat flux, gravity, volcanic front, mantle upwelling, ocean floor spreading

- Climate: sediment yield, modes of sediment transport, chemistry of deposits

Compressional uplift along master faults is probably needed for the dominance of axial sediment supply into the basin, which has the potential to produce and distribute huge volumes of detritus (Figure 15). Restraining bends as paired bends [12] such as in the Dead Sea Basin setting, and collision related to continental indentation such as in the Yinggehai Basin setting, are possible cases where axial sediment supply is enhanced. Conversely, a marginal high along the master fault is required for the formation of transpressional basins such as the Aceh Basin; therefore, marginal sediment supply may tend to dominate in such basins.

The continuous migration of depocenters requires that the progressive displacement of the master faults creates new accommodation space (Figure 15). In standard models of pull-apart basins, which are bounded by steep master faults and listric transverse faults, increasing the offset leads to a widening of the fault zone, resulting in wider pull-apart basins with a l/w ratio of about 3 for each basin [2, 42]. Therefore, for large l/w basins with continuous depocenter

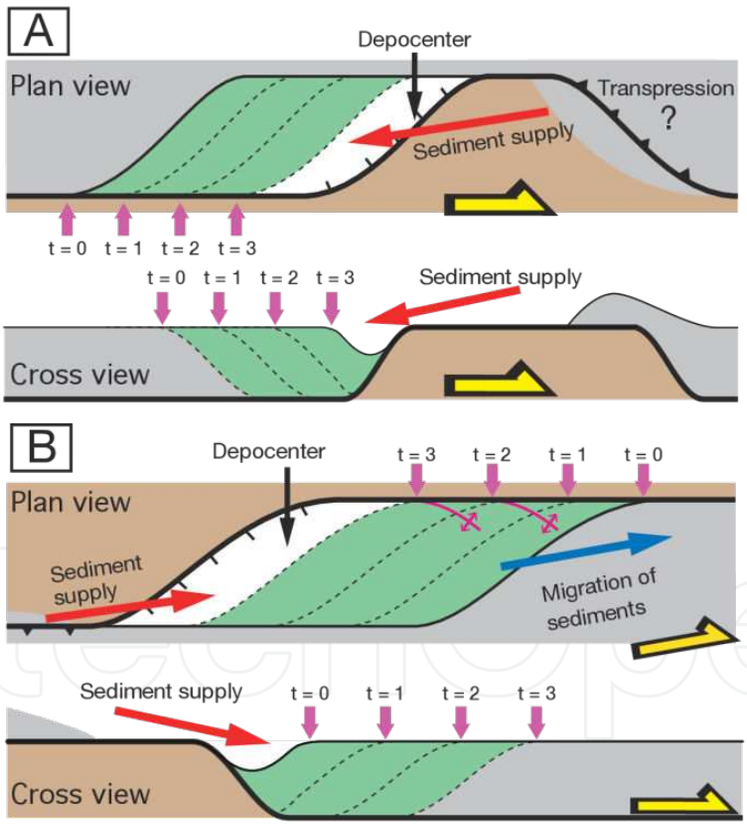

Figure 15. Conceptual models for depocenter migration and axial sediment supply in fault-bend basins. (A) Progressive right-lateral migration of paired bends on the foot-wall generates compressional uplift and extensional depression on the hanging-wall. Sediments are always supplied from the same direction along the long-axis of the basin. (B) Depocenter fixes along the releasing bend result from the right-lateral migration of sediments deposited on the foot-wall. A transpressional component would be required to generate the sediment source, and *en échelon* folds may form along the master faults. Both models generate deposits with axial sediments whose thicknesses are greater than the burial depths.

http://dx.doi.org/10.5772/56593

migration, such as the Dead Sea Basin and the Izumi Group, other formational mechanisms should be considered instead of the pull-apart basin model. Step-wise propagation or sequential progradation of the master fault could produce elongated stepover basins. A high *l*/*w* ratio could also potentially be produced by a transpressional basin along a trench-linked strike-slip fault. However, there is a need to establish physical models for basin formation in such settings.

Acknowledgements

Kai Berglar and his working groups kindly provided the bathymetric data of the Sumatra region. Financial support for this research was provided by the National Institute of Advanced Industrial Science and Technology (AIST). Constructive comments from Yasuto Itoh were insightful for improving the manuscript.

Author details

Atsushi Noda*

Address all correspondence to: a.noda@aist.go.jp

Geological Survey of Japan, National Institute of Advanced Industrial Science and Technology, Tsukuba, Ibaraki, Japan

References

[1] Nilsen TH, Mclaughlin RJ. Comparison of tectonic framework and depositional patterns of the Hornelen strike-slip basin of Norway and the Ridge and Little Sulphur Creek strike-slip basins of California. In: Biddle KT, Christie-Blick N (eds.) Strike-Slip Deformation, Basin Formation, and Sedimentation. Special Publication, no. 37. Tulsa, Oklahoma: SEPM; 1985. p. 79–103.

[2] Aydin A, Nur A. Evolution of pull-apart basins and their scale independence. Tectonics 1982;1(1) 91–105. doi:10.1029/TC001i001p00091.

[3] Noda A, Toshimitsu S. Backward stacking of submarine channel-fan successions controlled by strike-slip faulting: The Izumi Group (Cretaceous), southwest Japan. Lithosphere 2009;1(1) 41–59. doi:10.1130/L19.1.

[4] Nilsen TH, Sylvester AG. Strike-slip basins. In: Busby CJ, Ingersoll RV (eds.) Tectonics of Sedimentary Basins. Oxford: Blackwell Science; 1995. p. 425–457.

[5] Brothers DS, Driscoll NW, Kent GM, Harding AJ, Babcock JM, Baskin RL. Tectonic evolution of the Salton Sea inferred from seismic reflection data. Nature Geoscience 2009;2(8) 581–584. doi:10.1038/ngeo590.

[6] Dooley TP, Schreurs G. Analogue modelling of intraplate strike-slip tectonics: A review and new experimental results. Tectonophysics 2012;574–575 1–71. doi:10.1016/j.tecto.2012.05.030.

[7] Petrunin AG, Sobolev SV. Three-dimensional numerical models of the evolution of pull-apart basins. Physics of the Earth and Planetary Interiors 2008;171(1–4) 387–399. doi:10.1016/j.pepi.2008.08.017.

[8] Reading HG. Characteristics and recognition of strike-slip fault systems. In: Ballance PF, Reading HG (eds.) Sedimentation in Oblique-Slip Mobile Zones. International Association of Sedimentologists Special Publication, no. 4. Oxford: Blackwell Science; 1980. p. 7–26. doi:10.1002/9781444303735.ch2

[9] Woodcock NH, Daly MC. The role of strike-slip fault systems at plate boundaries and discussion. Philosophical Transactions of the Royal Society of London. Series A 1986;317(1539) 13–29. doi:10.1098/rsta.1986.0021.

[10] Christie-Blick N, Biddle KT. Deformation and basin formation along strike-slip faults. In: Biddle KT, Christie-Blick N (eds.) Strike-Slip Deformation, Basin Formation, and Sedimentation. Special Publication, no. 37. Tulsa, Oklahoma: SEPM; 1985. p. 1–34.

[11] Sylvester AG. Strike-slip faults. Geological Society of America Bulletin 1988;100(11) 1666–1703. doi:10.1130/0016-7606(1988)100<1666:SSF>2.3.CO;2.

[12] Mann P. Global catalogue, classification and tectonic origins of restraining-and releasing bends on active and ancient strike-slip fault systems. In: Cunningham WD, Mann P (eds.) Tectonics of strike-slip restraining and releasing bends. Special Publications, vol. 290, London: Geological Society; 2007. p. 13–142. doi:10.1144/SP290.2.

[13] Yeats RS, Sieh KE, Allen CR. Geology of Earthquakes. New York: Oxford University Press 1997, 576 pp.

[14] Fitch TJ. Plate convergence, transcurrent faults, and internal deformation adjacent to southeast Asia and the western Pacific. Journal of Geophysical Research 1972;77 4432–4460.

[15] Jarrard RD. Terrane motion by strike-slip faulting of forearc slivers. Geology 1986;14(9) 780–783. doi:10.1130/0091-7613(1986)14<780:TMBSFO>2.0.CO;2.

[16] McCaffrey R. Oblique plate convergence, slip vectors, and forearc deformation. Journal of Geophysical Research 1992;97(B6) 8905–8915.

[17] Carter K, Lerche I. Basin evolution, thermal history and hydrocarbon potential of the St. George Basin, Bering Sea, Alaska: A comparative study using one-and two-di-

mensional models. Marine and Petroleum Geology 1991;8(4) 392–409. doi: 10.1016/0264-8172(91)90062-6.

[18] Tsutsumi H, Okada A. Segmentation and Holocene surface faulting on the Median Tectonic Line, Southwest Japan. Journal of Geophysical Research 1996;101(B3) 5855–5871.

[19] Ikeda M, Toda S, Kobayashi S, Ohno Y, Nishizaka N, Ohno I. Tectonic model and fault segmentation of the Median Tectonic Line active fault system on Shikoku, Japan. Tectonics 2009;28(TC5006). doi:10.1029/2008TC002349.

[20] Karig DE, Lawrence MB, Moore GF, Curray JR. Structural frame work of the fore-arc basin, NW Sumatra. Journal of the Geological Society, London 1980;137(1) 77–91. doi: 10.1144/gsjgs.137.1.0077.

[21] McCaffrey R. The tectonic framework of the Sumatran subduction zone. Annual Review of Earth and Planetary Sciences 2009;37(1) 345–366. doi:10.1146/annurev.earth.031208.100212.

[22] Sieh K, Natawidjaja D. Neotectonics of the Sumatran fault, Indonesia. Journal of Geophysical Research 2000;105(B12) 28,295–28,326.

[23] Bruhn RL, Pavlis TL, Plafker G, Serpa L. Deformation during terrane accretion in the Saint Elias orogen, Alaska. Geological Society of America Bulletin 2004;116(7–8) 771–787. doi:10.1130/B25182.1.

[24] Berger AL, Spotila JA, Chapman JB, Pavlis TL, Enkelmann E, Ruppert NA, Buscher JT. Architecture, kinematics, and exhumation of a convergent orogenic wedge: A thermochronological investigation of tectonic–climatic interactions within the central St. Elias orogen, Alaska. Earth and Planetary Science Letters 2008;270(1–2) 13–24. doi: 10.1016/j.epsl.2008.02.034.

[25] Allen CR. Circum-Pacific faulting in the Philippines-Taiwan region. Journal of Geophysical Research 1962;67(4795). doi:10.1029/JZ067i012p04795.

[26] Bachman SB, Lewis SD, Schweller WJ. Evolution of a forearc basin, Luzon Central Valley, Philippines. American Association of Petroleum Geologists Bulletin 1983;67(7) 1143–1162. doi:10.1306/03B5B718-16D1-11D7-8645000102C1865D.

[27] Ryan HF, Coleman PJ. Composite transform-convergent plate boundaries: description and discussion. Marine and Petroleum Geology 1992;9(1) 89–97. doi: 10.1016/0264-8172(92)90006-Z.

[28] Förster H, Oles D, Knittel U, Defant MJ, Torres RC. The Macolod Corridor: A rift crossing the Philippine island arc. Tectonophysics 1990;183(1–4) 265–271. doi: 10.1016/0040-1951(90)90420-D.

[29] Ringenbach JC, Pinet N, Stéphan JF, Delteil J. Structural variety and tectonic evolution of strike-slip basins related to the Philippine Fault System, northern Luzon, Philippines. Tectonics 1993;12(1) 187–203. doi:10.1029/92TC01968.

[30] Coffin MF, Gahagan LM, Lawver p LA No 174. Present-day plate boundary digital data compilation. Technical Report 174, University of Texas Institute for Geophysics 1998.

[31] DeMets C, Gordon RG, Argus DF. Geologically current plate motions. Geophysical Journal International 2010;181(1) 1–80. doi:10.1111/j.1365-246X.2009.04491.x.

[32] Molnar P, Tapponnier P. Cenozoic tectonics of Asia: Effects of a continental collision: Features of recent continental tectonics in Asia can be interpreted as results of the India-Eurasia collision. Science 1975;189(4201) 419–426. doi:10.1126/science.189.4201.419.

[33] Zhang PZ. A review on active tectonics and deep crustal processes of the Western Sichuan region, eastern margin of the Tibetan Plateau. Tectonophysics 2013;584 7–22. doi:10.1016/j.tecto.2012.02.021.

[34] Barnes PM, Sutherland R, Delteil J. Strike-slip structure and sedimentary basins of the southern Alpine Fault, Fiordland, New Zealand. Geological Society of America Bulletin 2005;117 411–435.

[35] Wallace LM, Barnes P, Beavan J, Van Dissen R, Litchfield N, Mountjoy J, Langridge R, Lamarche G, Pondard N. The kinematics of a transition from subduction to strike-slip: An example from the central New Zealand plate boundary. Journal of Geophysical Research 2012;117(B02405). doi:10.1029/2011JB008640.

[36] Ballance PF, Reading HG (eds.) Sedimentation in Oblique-Slip Mobile Zones. International Association of Sedimentologists Special Publication, no. 4. Oxford: Blackwell Science; 1980. 265 pp. doi:10.1002/9781444303735

[37] Crowell JC, Link MH (eds.) Geologic History of Ridge Basin, Southern California. Los Angeles, California: SEPM, Pacific Section; 1982. 304 pp.

[38] Mann P, Hempton MR, Bradley DC, Burke K. Development of pull-apart basins. Journal of Geology 1983;91(5) 529–554.

[39] Hempton MR. The evolution of thought concerning sedimentation in pull-apart basins. In: Boardman SJ (ed.) In Revolution in the Earth Sciences: Advances in the Past Half-Century. Dubuque, Iowa: Kendall-Hunt Publishers; 1983. p. 167–180.

[40] Biddle KT, Christie-Blick N (eds.) Strike-Slip Deformation, Basin Formation, and Sedimentation. Special Publication, no. 37. Tulsa, Oklahoma: SEPM; 1985. 386 pp.

[41] Burchfiel BC, Stewart JH. "Pull-apart" origin of the central segment of Death Valley, California. Geological Society of America Bulletin 1966;77(4) 439–442. doi:10.1130/0016-7606(1966)77[439:POOTCS]2.0.CO;2.

[42] Basile C, Brun JP. Transtensional faulting patterns ranging from pull-apart basins to transform continental margins: an experimental investigation. Journal of Structural Geology 1999;21(1) 23–37. doi:10.1016/S0191-8141(98)00094-7.

[43] Zak I, Freund R. Asymmetry and basin migration in the dead sea rift. Tectonophysics 1981;80(1–4) 27–38. doi:10.1016/0040-1951(81)90140-2.

[44] Umhoefer PJ, Schwennicke T, Del Margo MT, Ruiz-Geraldo G, Ingle JC, McIntosh W. Transtensional fault-termination basins: An important basin type illustrated by the Pliocene San Jose Island basin and related basins in the southern Gulf of California, Mexico. Basin Research 2007;19(2) 297–322. doi:10.1111/j.1365-2117.2007.00323.x.

[45] Clift PD, Sun Z. The sedimentary and tectonic evolution of the Yinggehai–Song Hong basin and the southern Hainan margin, South China Sea: Implications for Tibetan uplift and monsoon intensification. Journal of Geophysical Research 2006;111(B06405). doi:10.1029/2005JB004048.

[46] Morley CK, Westaway R. Subsidence in the super-deep Pattani and Malay basins of Southeast Asia: a coupled model incorporating lower-crustal flow in response to post-rift sediment loading. Basin Research 2006;18(1) 51–84. doi:10.1111/j.1365-2117.2006.00285.x.

[47] Dorsey J Rebecca, Umhoefer J Paul. Influence of sediment input and plate-motion obliquity on basin development along an active oblique-divergent plate boundary: Gulf of California and Salton Trough. In: Busby C, Azor A (eds.) Tectonics of Sedimentary Basins: Recent Advances. Chap. 10. Chichester: Wiley-Blackwell; 2012. p. 209–225.

[48] Mann P. Model for the formation of large, transtensional basins in zones of tectonic escape. Geology 1997;25(3) 211–214. doi:10.1130/0091-7613(1997)025<0211:MFTFOL>2.3.CO;2.

[49] Koukouvelas IK, Aydin A. Fault structure and related basins of the North Aegean Sea and its surroundings. Tectonics 2002;21(1046). doi:10.1029/2001TC901037.

[50] Itoh Y, Takemura K, Kamata H. History of basin formation and tectonic evolution at the termination of a large transcurrent fault system: deformation mode of central Kyushu, Japana. Tectonophysics 1998;284(1–2) 135–150. doi:10.1016/S0040-1951(97)00167-4.

[51] Cabrera L, Roca E, Santanach P. Basin formation at the end of a strike-slip fault: the Cerdanya Basin (eastern Pyrenees). Journal of the Geological Society, London 1988;145(2) 261–268. doi:10.1144/gsjgs.145.2.0261.

[52] Beaumont C. Foreland basins. Geophysical Journal of the Royal Astronomical Society 1981;65(2) 291–329. doi:10.1111/j.1365-246X.1981.tb02715.x.

[53] DeCelles PG, Giles KA. Foreland basin systems. Basin Research 1996;8(2) 105–123. doi:10.1046/j.1365-2117.1996.01491.x.

[54] Sinclair HD, Naylor M. Foreland basin subsidence driven by topographic growth versus plate subduction. Geological Society of America Bulletin 2012;124(3–4) 368–379. doi:10.1130/B30383.1.

[55] Crowell JC (ed.) Evolution of Ridge Basin, Southern California: An Interplay of Sedimentation and Tectonics. Special Paper 367. Boulder, Colorado: Geological Society of America; 2003. 247 pp.

[56] May SR, Ehman KD, Gray GG, Crowell JC. A new angle on the tectonic evolution of the Ridge Basin, a "strike-slip" basin in Southern California. Geological Society of America Bulletin 1993;105(10) 1357–1372. doi: 10.1130/0016-7606(1993)105<1357:ANAOTT>2.3.CO;2.

[57] Link MH. Depositional systems and sedimentary facies of the Miocene-Pliocene Ridge Basin Group, Ridge Basin, southern California. In: Crowell JC (ed.) Evolution of Ridge Basin, Southern California: An Interplay of Sedimentation and Tectonics. Special Paper 367. Boulder, Colorado: Geological Society of America; 2003. p. 17–87. doi:10.1130/0-8137-2367-1.17.

[58] Crowell JC. Introduction to geology of Ridge Basin, Southern California. In: Crowell JC (ed.) Evolution of Ridge Basin, Southern California: An Interplay of Sedimentation and Tectonics. Special Paper 367. Boulder, Colorado: Geological Society of America; 2003. p. 1–15. doi:10.1130/0-8137-2367-1.1.

[59] Crowell JC. Tectonics of Ridge Basin region, southern California. In: Crowell JC (ed.) Evolution of Ridge Basin, Southern California: An Interplay of Sedimentation and Tectonics. Special Paper 367. Boulder, Colorado: Geological Society of America; 2003. p. 157–203. doi:10.1130/0-8137-2367-1.157.

[60] Link MH, Smith PR. Organic geochemistry of Ridge Basin, southern California. In: Crowell JC, Link MH (eds.) Geologic History of Ridge Basin, Southern California. Los Angeles, California: SEPM, Pacific Section; 1982. p. 191–197.

[61] Crowell JC. The tectonics of Ridge Basin, southern California. In: Crowell JC, Link MH (eds.) Geologic History of Ridge Basin, Southern California. Los Angeles, California: SEPM, Pacific Section; 1982. p. 25–42.

[62] Weber M, Abu-Ayyash K, Abueladas A, Agnon A, Alasonati-Tasárová Z, Al-Zubi H, Babeyko A, Bartov Y, Bauer K, Becken M, Bedrosian PA, Ben-Avraham Z, Bock G, Bohnhoff M, Bribach J, Dulski P, Ebbing J, El-Kelani R, Föster A, Förster HJ, Frieslander U, Garfunkel Z, Goetze HJ, Haak V, Haberland C, Hassouneh M, Helwig S, Hofstetter A, Hoffmann-Rothe A, Jäckel KH, Janssen C, Jaser D, Kesten D, Khatib M, Kind R, Koch O, Koulakov I, Laske G, Maercklin N, Masarweh R, Masri A, Matar A, Mechie J, Meqbel N, Plessen B, Möller P, Mohsen A, Oberhänli R, Oreshin S, Petrunin A, Qabbani I, Rabba I, Ritter O, Romer RL, Rümpker G, Rybakov M, Ryberg T, Saul J, Scherbaum F, Schmidt S, Schulze A, Sobolev SV, Stiller M, Stromeyer D, Tarawneh K, Trela C, Weckmann U, Wetzel U, Wylegalla K. Anatomy of the Dead Sea

Transform from lithospheric to microscopic scale. Reviews of Geophysics 2009;47(RG2002). doi:10.1029/2008RG000264.

[63] Lazar M, Ben-Avraham Z, Schattner U. Formation of sequential basins along a strike–slip fault–Geophysical observations from the Dead Sea basin. Tectonophysics 2006;421(1–2) 53–69. doi:10.1016/j.tecto.2006.04.007.

[64] Garfunkel Z, Ben-Avraham Z. The structure of the Dead Sea basin. Tectonophysics 1996;266(1–4) 155–176. doi:10.1016/S0040-1951(96)00188-6.

[65] Ben-Avraham Z, Lyakhovsky V, Schubert G. Drop-down formation of deep basins along the Dead Sea and other strike-slip fault systems. Geophysical Journal International 2010;181(1) 185–197. doi:10.1111/j.1365-246X.2010.04525.x.

[66] Ben-Avraham Z, Schubert G. Deep "drop down" basin in the southern Dead Sea. Earth and Planetary Science Letters 2006;251(3–4) 254–263. doi:10.1016/j.epsl.2006.09.008.

[67] ten Brink US, Ben-Avraham Z. The anatomy of a pull-apart basin: Seismic reflection observations of the Dead Sea Basin. Tectonics 1989;8(2) 333–350.

[68] Ben-Avraham Z, Hänel R, Villinger H. Heat flow through the Dead Sea rift. Marine Geology 1978;28(3–4) 253–269. doi:10.1016/0025-3227(78)90021-X.

[69] Hurwitz S, Garfunkel Z, Ben-Gai Y, Reznikov M, Rotstein Y, Gvirtzman H. The tectonic framework of a complex pull-apart basin: seismic reflection observations in the Sea of Galilee, Dead Sea transform. Tectonophysics 2002;359(3–4) 289–306. doi:10.1016/S0040-1951(02)00516-4.

[70] Heimann A, Zilberman E, Amit R, Frieslander U. Northward migration of the southern diagonal fault of the Hula pull-apart basin, Dead Sea Transform, northern Israel. Tectonophysics 2009;476(3–4) 496–511. doi:10.1016/j.tecto.2009.07.024.

[71] Greenbaum N, Ben-Zvi A, Haviv I, Enzel Y. The hydrology and paleohydrology of the Dead Sea tributaries. In: Enzel Y, Agnon A, Stein M (eds.) New Frontiers in Dead Sea Paleoenvironmental Research. Special Paper 401. Boulder, Colorado: Geological Society of America; 2006. p. 63–93. doi:10.1130/2006.2401(05).

[72] Bartov Y, Bookman R, Enzel Y. Current depositional environments at the Dead Sea margins as indicators of past lake levels. In: Enzel Y, Agnon A, Stein M (eds.) New Frontiers in Dead Sea Paleoenvironmental Research. Special Paper 401. Boulder, Colorado: Geological Society of America; 2006. p. 127–140. doi:10.1130/2006.2401(08).

[73] Zhang Q, Zhang Q. A distinctive hydrocarbon basin—Yinggehai Basin, South China Sea. Journal of Southeast Asian Earth Sciences 1991;6(2) 69–74. doi:10.1016/0743-9547(91)90097-H.

[74] Nielsen LH, Mathiesen A, Bidstrup T, VejbÃęk OV, Dien PT, Tiem PV. Modelling of hydrocarbon generation in the Cenozoic Song Hong Basin, Vietnam: a highly pro-

spective basin. Journal of Asian Earth Sciences 1999;17(1–2) 269–294. doi:10.1016/S0743-9547(98)00063-4.

[75] Tapponnier P, Peltzer G, Armijo R. On the mechanics of the collision between India and Asia. In: Coward MP, Alison C (eds.) Collision Tectonics. Special Publications, vol. 19. London: Geological Society; 1986. p. 113–157. doi:10.1144/GSL.SP.1986.019.01.07.

[76] Tapponnier P, Lacassin R, Leloup P, Scharer U, Dalai Z, Haiwei W, Xiaohan L, Shaocheng J, Lianshang Z, Jiayou Z. The Ailao Shan/Red River metamorphic belt: Tertiary left-lateral shear between. Nature 1990;343(6257) 431–437. doi:10.1038/343431a0.

[77] Rangin C, Klein M, Roques D, Le Pichon X, Trong LV. The Red River fault system in the Tonkin Gulf, Vietnam. Tectonophysics 1995;243(3–4) 209–222. doi:10.1016/0040-1951(94)00207-P.

[78] Leloup PH, Lacassin R, Tapponnier P, Schärer U, Zhong D, Liu X, Zhang L, Ji S, Trinh PT. The Ailao Shan-Red River shear zone (Yunnan, China), Tertiary transform boundary of Indochina. Tectonophysics 1995;251(1–4) 3–84. doi:10.1016/0040-1951(95)00070-4.

[79] Leloup PH, Arnaud N, Lacassin R, Kienast JR, Harrison TM, Trong TTP, Replumaz A, Tapponnier P. New constraints on the structure, thermochronology, and timing of the Ailao Shan-Red River shear zone, SE Asia. Journal of Geophysical Research 2001;106(6683). doi:10.1029/2000JB900322.

[80] Zhu M, Graham S, Mchargue T. The Red River Fault zone in the Yinggehai Basin, South China Sea. Tectonophysics 2009;476(3–4) 397–417. doi:10.1016/j.tecto.2009.06.015.

[81] Allen CR, Gillespie AR, Yuan H, Sieh KE, Buchun Z, Chengnan Z. Red River and associated faults, Yunnan Province, China: Quaternary geology, slip rates, and seismic hazard. Geological Society of America Bulletin 1984;95(6) 686–700. doi:10.1130/0016-7606(1984)95<686:RRAAFY>2.0.CO;2.

[82] Replumaz A, Lacassin R, Tapponnier P, Leloup PH. Large river offsets and Plio-Quaternary dextral slip rate on the Red River fault (Yunnan, China). Journal of Geophysical Research 2001;106(819). doi:10.1029/2000JB900135.

[83] Schoenbohm LM, Burchfiel BC, Liangzhong C, Jiyun Y. Miocene to present activity along the Red River fault, China, in the context of continental extrusion, upper-crustal rotation, and lower-crustal flow. Geological Society of America Bulletin 2006;118(5–6) 672–688. doi:10.1130/B25816.1.

[84] Tapponnier P, Peltzer G, Le Dain AY, Armijo R, Cobbold P. Propagating extrusion tectonics in Asia: New insights from simple experiments with plasticine. Geology 1982;10(12) 611–616. doi:10.1130/0091-7613(1982)10<611:PETIAN>2.0.CO;2.

[85] Lee TY, Lawver LA. Cenozoic plate reconstruction of Southeast Asia. Tectonophysics 1995;251(1–4) 85–138. doi:10.1016/0040-1951(95)00023-2.

[86] Guo L, Zhong Z, Wang L, Shi Y, Li H, Liu S. Regional tectonic evolution around Yinggehai basin of South China Sea. Geological Journal of China University 2001;7(1) 1–12.

[87] Li S, Lin C, Zhang Q, Yang S, Wu P. Episodic rifting of continental marginal basins and tectonic events since 10 Ma in the South China Sea. Chinese Science Bulletin 1999;44(1) 10–23. doi:10.1007/BF03182877.

[88] Sun Z, Zhou D, Zhong Z, Zeng Z, Wu S. Experimental evidence for the dynamics of the formation of the Yinggehai basin, NW South China Sea. Tectonophysics 2003;372(1–2) 41–58. doi:10.1016/S0040-1951(03)00230-0.

[89] Luo X, Dong W, Yang J, Yang W. Overpressuring mechanisms in the Yinggehai Basin, South China Sea. American Association of Petroleum Geologists Bulletin 2003;87(4) 629–645. doi:10.1306/10170201045.

[90] Lei C, Ren J, Clift PD, Wang Z, Li X, Tong C. The structure and formation of diapirs in the Yinggehai–Song Hong Basin, South China Sea. Marine and Petroleum Geology 2011;28(5) 980–991. doi:10.1016/j.marpetgeo.2011.01.001.

[91] Zhong Z, Wang L, Xia B, Dong W, Sun Z, Shi Y. The dynamics of Yinggehai Basin Formation and its tectonic significance. Acta Geologica Sinica 2004;78(3) 302–309. (in Chinese with English abstract).

[92] Yan Y, Carter A, Palk C, Brichau S, Hu X. Understanding sedimentation in the Song Hong–Yinggehai Basin, South China Sea. Geochemistry, Geophysics, Geosystems 2011;12(Q06014). doi:10.1029/2011GC003533.

[93] He L, Xiong L, Wang J. Heat flow and thermal modeling of the Yinggehai Basin, South China Sea. Tectonophysics 2002;351(3) 245–253. doi:10.1016/S0040-1951(02)00160-9.

[94] Ngah K, Madon M, Tjia HD. Role of pre-Tertiary fractures in formation and development of the Malay and Penyu basins. In: Hall R, Blundell D (eds.) Tectonic Evolution of Southeast Asia. Special Publications, vol. 106. London: Geological Society; 1996. p. 281–289. doi:10.1144/GSL.SP.1996.106.01.18.

[95] Morley CK. A tectonic model for the Tertiary evolution of strike–slip faults and rift basins in SE Asia. Tectonophysics 2002;347(4) 189–215. doi:10.1016/S0040-1951(02)00061-6.

[96] Searle MP, Morley CK. Tectonic and thermal evolution of Thailand in the regional context of SE Asia. In: Ridd MF, Barber AJ, Crow MJ (eds.) The Geology of Thailand, Chap. 20. London: Geological Society; 2011. p. 539–571.

[97] Fyhn MBW, Boldreel LO, Nielsen LH. Escape tectonism in the Gulf of Thailand: Paleogene left-lateral pull-apart rifting in the Vietnamese part of the Malay Basin. Tectonophysics 2010;483(3–4) 365–376. doi:10.1016/j.tecto.2009.11.004.

[98] Miall AD. Architecture and Sequence Stratigraphy of Pleistocene Fluvial Systems in the Malay Basin, Based on Seismic Time-Slice Analysis. American Association of Petroleum Geologists Bulletin 2002;86(7) 1201–1216. doi:10.1306/61EEDC56-173E-11D7-8645000102C1865D.

[99] Madon MB, Watts. Gravity anomalies, subsidence history and the tectonic evolution of the Malay and Penyu Basins (offshore Peninsular Malaysia). Basin Research 1998;10(4) 375–392. doi:10.1046/j.1365-2117.1998.00074.x.

[100] Petersen HI, Mathiesen A, Fyhn MBW, Dau NT, Bojesen-Koefoed JA, Nielsen LH, Nytoft HP. Modeling of petroleum generation in the Vietnamese part of the Malay Basin using measured kinetics. American Association of Petroleum Geologists Bulletin 2011;95(4) 509–536. doi:10.1306/09271009171.

[101] Watcharanantakul R, Morley CK. Syn-rift and post-rift modelling of the Pattani Basin, Thailand: evidence for a ramp-flat detachment. Marine and Petroleum Geology 2000;17(8) 937–958. doi:10.1016/S0264-8172(00)00034-9.

[102] Ghosal D, Singh SC, Chauhan APS, Hananto ND. New insights on the offshore extension of the Great Sumatran fault, NW Sumatra, from marine geophysical studies. Geochemistry, Geophysics, Geosystems 2012;13. doi:10.1029/2012GC004122.

[103] Izart A, Mustafa Kemal B, Malod JA. Seismic stratigraphy and subsidence evolution of the Northwest Sumatra fore-arc basin. Marine Geology 1994;122(1–2) 109–124. doi:10.1016/0025-3227(94)90207-0.

[104] Berglar K, Gaedicke C, Lutz R, Franke D, Djajadihardja YS. Neogene subsidence and stratigraphy of the Simeulue forearc basin, Northwest Sumatra. Marine Geology 2008;253(1–2) 1–13. doi:10.1016/j.margeo.2008.04.006.

[105] Berglar K, Gaedicke C, Franke D, Ladage S, Klingelhoefer F, Djajadihardja YS. Structural evolution and strike-slip tectonics off north-western Sumatra. Tectonophysics 2010;480(1–4) 119–132. doi:10.1016/j.tecto.2009.10.003.

[106] Seeber L, Mueller C, Fujiwara T, Arai K, Soh W, Djajadihardja YS, Cormier MH. Accretion, mass wasting, and partitioned strain over the 26 Dec 2004 Mw9.2 rupture offshore Aceh, northern Sumatra. Earth and Planetary Science Letters 2007;263(1–2) 16–31. doi:10.1016/j.epsl.2007.07.057.

[107] Curray JR. Tectonics and history of the Andaman Sea region. Journal of Asian Earth Sciences 2005;25(1) 187–232. doi:10.1016/j.jseaes.2004.09.001.

[108] Henstock TJ, Mcneill LC, Tappin DR. Seafloor morphology of the Sumatran subduction zone: Surface rupture during megathrust earthquakes? Geology 2006;34(6) 485–488. doi:10.1130/22426.1.

[109] Graindorge D, Klingelhoefer F, Sibuet JC, Mcneill L, Henstock TJ, Dean S, Gutscher MA, Dessa JX, Permana H, Singh SC, Leau H, White N, Carton H, Malod JA, Rangin C, Aryawan KG, Chaubey AK, Chauhan A, Galih DR, Greenroyd CJ, Laesanpura A, Prihantono J, Royle G, Shankar U. Impact of lower plate structure on upper plate deformation at the NW Sumatran convergent margin from seafloor morphology. Earth and Planetary Science Letters 2008;275(3–4) 201–210. doi:10.1016/j.epsl.2008.04.053.

[110] Dean SM, Mcneill LC, Henstock TJ, Bull JM, Gulick SPS, Austin JA, Bangs NLB, Djajadihardja YS, Permana H. Contrasting Décollement and Prism Properties over the Sumatra 2004–2005 Earthquake Rupture Boundary. Science 2010;329(5988) 207–210. doi:10.1126/science.1189373.

IntechOpen